Neuropharmacology 162 (2020) 107829

Contents lists available at ScienceDirect

Neuropharmacology

journal homepage: www.elsevier.com/locate/neuropharm

Genetic deletion of GPR88 enhances the locomotor response to L-DOPA in experimental parkinsonism while counteracting the induction of dyskinesia

Ioannis Mantas[a,**], Yunting Yang[a], Clotilde Mannoury-la-cour[b], Mark J. Millan[b], Xiaoqun Zhang[a], Per Svenningsson[a,*]

[a] Department of Clinical Neuroscience, Karolinska Institutet, Stockholm, Sweden
[b] Centre for Therapeutic Innovation-CNS, Institut de Recherches Servier, Centre de Recherches de Croissy, Paris, France

HIGHLIGHTS

- GPR88 KO exhibit an enhanced locomotor response but lowered dyskinesia to L-DOPA.
- GPR88 KO mice show altered L-DOPA induced mRNA changes.
- GPR88 KO mice display a reduction in tacrine-mediated PD-like tremor.
- GPR88 has an active role in regulating striatal glutamate and serotonin.

ARTICLE INFO

Keywords:
Parkinsonism
GPR88
Glutamate release
L-DOPA
Dyskinesia
Rotations
6hydroxydopamine

ABSTRACT

Parkinson's disease (PD) is characterized by progressive loss of midbrain dopaminergic neurons and treated with the dopamine precursor, 3,4-dihydroxy-L-phenylalanine (L-DOPA). Prolonged L-DOPA treatment is however associated with waning efficacy and the induction of L-DOPA induced dyskinesia (LID). GPR88 is an orphan G-protein Coupled Receptor (GPCR) expressed in dopaminoceptive striatal medium spiny neurons (MSNs) and their afferent corticostriatal glutamatergic neurons. Here, we studied the role of GPR88 in experimental parkinsonism and LID. Chronic L-DOPA administration to male GPR88 KO mice, subjected to unilateral 6-hydroxydopamine (6-OHDA) lesions of the medial forebrain bundle, resulted in more rotations than in their WT counterparts. Conversely, GPR88 KO mice had a lower abnormal involuntary movements (AIMs) score. These behavioral responses were accompanied by altered transcription of L-DOPA upregulated genes in lesioned GPR88 KO compared to WT striata. In accordance with a role for serotonin neurons in LID development, WT but not GPR88 KO striata exhibited 5-hydroxytryptamine displacement upon repeated L-DOPA treatment. Intact male GPR88 KO mice showed diminished tacrine-induced PD-like tremor and spontaneous hyperlocomotion. Dopamine and its metabolites were not increased in male GPR88 KO mice, but biosensor recordings revealed increased spontaneous/basal and evoked glutamate release in striata of male GPR88 KO mice. In conclusion, genetic deletion of GPR88 promotes L-DOPA-induced rotation and spontaneous locomotion yet suppresses the induction of LIDs and also reduces tremor. These data provide behavioral, neurochemical and molecular support that GPR88 antagonism may favour motor relief in PD patients without aggravating the induction of motor side effects.

1. Introduction

Parkinson's disease (PD) is diagnosed based on the occurrence of bradykinesia, rigidity and tremor (Postuma et al., 2015). However, PD symptomatology extends beyond the motor deficits and includes psychiatric symptoms, autonomic dysfunction, sleep disturbances, cognitive impairment and hyposmia (Poewe et al., 2017). Disruption of motor function is principally caused by the progressive loss of the dopamine (DA) producing neurons of the substantia nigra pars compacta (SNc) (Bernheimer et al., 1973). Symptomatic treatment in PD aims at restoring DA neurotransmission by stimulating DA D2 receptors (D2R), inhibiting monoamine oxidase B or catechol-o-methyltransferase, and/or administering 3, 4-dihydroxy-L-phenylalanine (L-DOPA) which is decarboxylated to DA (Poewe et al., 2017). The major postsynaptic

* Corresponding author.
** Corresponding author.
E-mail addresses: ioannis.mantas@ki.se (I. Mantas), per.svenningsson@ki.se (P. Svenningsson).

https://doi.org/10.1016/j.neuropharm.2019.107829
Received 24 August 2019; Received in revised form 20 October 2019; Accepted 22 October 2019
Available online 24 October 2019

Abbreviations

PD	Parkinson's disease
GPCR	G-protein coupled receptor
L-DOPA	3,4-dihydroxy-L-phenylalanine
LID	L-DOPA induced dyskinesia
MSNs	Medium spiny neurons
6-OHDA	6-hydroxydopamine
AIMs	Abnormal involuntary movements
DA	Dopamine
SNc	Substantia nigra pars compacta
D1/2R	D1/2 receptors
PDYN	Prodynorphin
PENK	Preproenkephalin
MFB	Medial forebrain bundle
KO	Knock-out
FAST	Fast analytical sensing technology
DAT	Dopamine transporter
ISH	In situ hybridization
ARC	Activity-regulated cytoskeleton-associated protein
GAD67	Glutamate decarboxylase 67
HPLC	High-performance liquid chromatography
ECD	Electrochemical detection
NA	Noradrenaline
DOPAC	3,4-Dihydroxyphenylacetic acid
5-HIAA	5-hydroxyindole-3-acetic acid
HVA	Homovanillic acid
5-HT	5-hydroxytryptamine
3-MT	3-methoxytyramine
VMA	Vanillylmandelic acid
EPI	Epinephrine
DOPA	Dihydroxyphenylalanine
MHPG	3-methoxy-4-hydroxyphenylglycol
EDTA	Ethylene-diamine-tetra-acetic acid
OSA	1-octanesulfonic acid
TEA	Triethylamine
PCA	Perchloric acid
MEAs	microelectrode arrays
AUC	Area under curve
T80	80% decay
CINs	Cholinergic interneurons
TJM	Tremulous jaw movements
LTP	Long term potentiation
LTD	Long term depression

targets of SNc neurons are the striatal GABAergic medium spiny neurons (MSNs). The MSNs are divided in two distinct neurochemical and anatomical subpopulations: the prodynorphin (PDYN)/D1R+ neurons projecting directly to substantia nigra pars reticulata and the preproenkephalin (PENK)/D2R+ neurons projecting indirectly to substantia nigra pars reticulate via relays in the globus pallidus and the subthalamic nucleus (Gerfen and Surmeier, 2011). Furthermore, these MSN subtypes have different involvement in motor programs as increased activity of PDYN/D1R+ neurons, but reduced activity of PENK/D2R+ neurons, stimulates locomotor activity (Bamford et al., 2018). Elevated levels of DA in the dorsal striatum following L-DOPA administration enhance locomotor activity via both the striatal output pathways (Bamford et al., 2018). Unfortunately, repeated administration L-DOPA often leads to involuntary movements referred as LDOPA induced dyskinesias (LIDs) (Cenci et al., 1998; Poewe et al., 2017).

A common method to cause DA depletion and induce experimental parkinsonism is to unilaterally inject 6-hydroxydopamine (6-OHDA) within the medial forebrain bundle (MFB) (Ungerstedt and Arbuthnott, 1970; Schober, 2004). This model is often used to study anti-parkinsonian as well as dyskinetic actions of L-DOPA and other dopaminomimetic compounds (Cenci et al., 1998).

The orphan GPCR, GPR88, is a potential therapeutic target against PD (Mizushima et al., 2000; Alavi et al., 2018). Thus, in situ hybridization analysis of GPR88 mRNA has demonstrated predominant expression in the striatum and moderate levels of the transcript in the olfactory tubercle, the inferior olivary nucleus, amygdala and cerebral cortex (Mizushima et al., 2000; Massart et al., 2009). Subcellular localization studies showed that GPR88 is highly expressed in both MSN populations in dendritic spines at proximity to corticostriatal synapses (Massart et al., 2009), Deletion of GPR88 in mice leads to hyperactivity and foraging deficiency due to the enhanced basal firing rate of MSNs associated with a facilitation of AMPA receptors signaling (Quintana et al., 2012; Rainwater et al., 2017). Using the unilateral 6-OHDA model, it has previously been showed that 6-OHDA lesions led to opposite changes in GPR88 expression in the two MSN populations which were reversed by chronic administration of L-DOPA (Massart et al., 2009).

Based on the abovementioned findings, we hypothesized that GPR88 may play an important role in PD and in modulating L-DOPA responses. We therefore used GPR88 wild type (WT) and knock-out (KO) mice to investigate the functional implications of GPR88 in several PD related conditions. First, we evaluated the influence of GPR88 on the anti-parkinsonian and dyskinetic side effect of LDOPA treatment. For this experiment, we used the unilateral 6-OHDA lesion model in both GPR88 WT and KO mice and studied rotational and dyskinetic behaviours upon repeated L-DOPA administration. Second, we analysed the DA transporter (DAT) protein, monoamines and their metabolites as well as key neuroplastic genes of MSNs in unilaterally 6-OHDA lesioned GPR88 WT and KO mice which had undergone chronic L-DOPA treatment. Third, we examined the responses of GPR88 WT and KO mice towards tacrine-induced PD-like tremor. Fourth, we assessed spontaneous locomotion in GPR88 WT and KO mice. Fifth, since GPR88 KO mice exhibit spontaneous hyperlocomotion in a DA-independent manner and GPR88 is anatomically positioned to modulate the corticostriatal glutamate transmission, we performed fast analytical sensing technology (FAST) measures of glutamate in striata of GPR88 WT and KO mice.

2. Materials and methods

2.1. Animals

Adult male GPR88 WT and KO mice on a C57Bl6J background were provided by Charles River. They were housed in temperature- and humidity-controlled rooms (20 °C, 53% humidity) with a 12 h dark/light cycle. The mice had access to standard food pellets and water ad libitum. The experiments were approved by the local ethical committee at Karolinska Institute (15191-2017) and conducted in accordance with the European Communities Council Directive of 24 November 1986 (86/609/EEC).

2.2. Experiments performed in unilaterally 6-OHDA-lesioned GPR88 WT and KO mice

2.2.1. 6-OHDA lesioning and treatment

15 WT and 16 KO male mice were anesthetized with 80 mg/kg ketamine (i.p.; Parke-Davis) and 5 mg/kg xylazine (i.p.; Bayer), pretreated with 25 mg/kg desipramine (i.p.; Sigma–Aldrich) and 5 mg/kg pargyline (i.p.; Sigma–Aldrich), placed in a stereotaxic frame, and injected, over 2 min, with 3 μg of 6-OHDA in 0.01% ascorbate (Sigma–Aldrich) into the median forebrain bundle (MFB) of the right hemisphere. The coordinates for injection were AP, −1.1 mm; ML,

−1.1 mm; and DV, −4.75 mm relative to bregma and the dural surface (Paxinos and Franklin, 2001). Two weeks after unilateral 6-OHDA administration, we validated the lesion by treating the mice with 1 mg/kg apomorphine (i.p; Sigma–Aldrich) and assessed rotational behavior. All mice rotated contralaterally and none of them was excluded from the study. Four weeks after surgery, mice were treated with saline or 10/7.5 mg/kg LDOPA/benserazide (i.p.; Sigma–Aldrich) once daily for 21 days. Animals were killed 1 h after the last injection. For brevity, L-DOPA/benserazide treatments are solely labelled L-DOPA throughout this article.

2.2.2. Measurements of rotations and abnormal involuntary movements (AIMs)

For measurements of rotations and AIMs, unilaterally 6-OHDA-lesioned mice were treated with LDOPA and placed in individual cages. The number of ipsilateral and contralateral rotations was thereafter counted for 30 min on days 1, 7, 14 and 21 to measure motor responses to L-DOPA, which are known to supersensitize upon chronic L-DOPA administration (Bibbiani et al., 2001). Immediately after the quantification of rotational behaviors, the incidence of AIMs was scored for 5 min (Zhang et al., 2008). This procedure was adapted from a validated rodent scale (Lundblad et al., 2004). The AIMs were classified into four subtypes: Forelimb, Orofacial, Axial, and Locomotive behaviors. Enhanced manifestations of normal behaviors such as grooming, gnawing, rearing, and sniffing were not included in the rating. The severity of each AIM subtype was assessed using scores from 0 to 4 (0: absent, 1: occasional, i.e., present less than 50% of the time; 2: frequent, i.e., present more than 50% of the time; 3: continuous, but interrupted by strong sensory stimuli and 4: continuous, not interrupted by strong sensory stimuli).

2.2.3. Autoradiographic detection of the DA transporter (DAT)

This method was used as an additional validation of the lesioning described in section 2.2.1. Slides mounted fresh frozen sections (12 μm thick) at the level of striatum were preincubated in 50 mM Tris–HCl/120 mM NaCl (pH 7.5) for 20 min. Incubation in binding buffer (50 mM Tris– HCl/120 mM NaCl, pH 7.5/1 μM fluoxetine) was conducted with 50 pM of the DAT ligand (125I) RTI55 (PerkinElmer Life Sciences, Boston, USA) for 60 min. To detect nonspecific binding, 100 μM nomifensine was added to the assay. The slides were washed 2 × 10 s in ice-cold binding buffer, rapidly dipped in deionized water, dried, and exposed to autoradiographic films (BioMax MR, Merck Eurolab, Sweden) in X-ray cassettes at −20 °C for 7 days before being developed (Kodak D19, Unifix).

2.2.4. In situ hybridization (ISH) experiments

In situ hybridization was performed in cryostat (Leica CM 3050 S) fresh frozen sections (12 μm thick) as previously described (Svenningsson et al., 1997). Briefly, 35S-labelled anti-sense and sense cRNA probes were prepared by in vitro transcription from cDNA clones corresponding to fragments of activity-regulated cytoskeleton-associated protein (ARC), proenkephalin (PENK), prodynorphin (PDYN) and glutamate decarboxylase 67 (GAD67). The transcription was performed from 50 to 100 ng of linearized plasmid using (35S) UTP (1000 Ci/mmol) and SP6, T3, T7 RNA polymerase. Cryostat sections were post fixed in 4% PFA for 5 min at room temperature, rinsed twice in 4 × sodium chloride–sodium citrate buffer (SSC) and placed into 0.25% acetic anhydride in 0.1 M triethanolamine/4 × SSC (pH 8) for 10 min at room temperature. After dehydration in graded alcohols, the sections were hybridized overnight at 55 °C with 35S-labelled probe in 50 μl of hybridization solution (20 mM Tris–HCl/1 mM EDTA/300 mM NaCl/50% formamide/10% dextran sulphate/1 × Denhardt's/250 μg/ml yeast tRNA/100 μg/ml salmon sperm DNA/0.1% SDS/0.1% sodium thiosulphate). The slides were washed in 4 × SSC (5 min, four times), RNAse A (20 μg/ml) (20 min, at 37 °C), 2 × SSC (5 min, twice), 1 × SSC(5 min), 0.5 × SSC (5 min) at room temperature, and rinsed in 0.1 × SSC at 65 °C (30 min, twice) (all washes contained 1 mM DTT), before being dehydrated in graded alcohols. The slides were then exposed on X-ray films for four to 28 days.

Fluorescent ISH (RNAscope) were performed using the RNAscope Multiplex Fluorescent Assay (Advanced Cell Diagnostics). Cryostat (Leica CM 3050 S) fresh frozen sections (12 μm thick) were post fixed in 4% PFA for 15 min at 4 °C and dehydrated in graded alcohols. Afterwards, it was applied Protease IV (Advanced Cell Diagnostics) for 30 min at room temperature. Then, the sections were hybridized with the probes: Pdyn (Mm-Pdyn-C3, cat. 318771-C3) and Arc (Mm-ArcC2, cat. 316911-C2) for 2 h at 40 °C. The hybridization step was followed by standardized steps of amplification (Amp 1-FL 30 min at 40 °C, Amp 2-FL 15 min at 40 °C, Amp 3-FL 30 min at 40 °C, Amp 4C-FL 15 min at 40 °C). After the last amplification step the sections where counterstained with DAPI (Advanced Cell Diagnostics) and mounted with Dako fluorescent mounting medium. Sections were imaged on a Carl Zeiss LSM 880 confocal microscope using a 63 × 1.4 NA oil immersion objective. Z-stacks of 5–7 μm thickness were obtained in each caption.

2.2.5. Analysis of neurotransmitters in mouse brain by HPLC

Methods for sample preparation and high-performance liquid chromatography (HPLC) with electrochemical detection (ECD) were based on two previously published protocols (Hubbard et al., 2010; Yang and Beal, 2011) and are described in detail below.

Chemicals and reagents: L-Noradrenaline hydrochloride (NA), 3,4-Dihydroxyphenylacetic acid (DOPAC), dopamine hydrochloride (DA), 5-hydroxyindole-3-acetic acid (5-HIAA), homovanillic acid (HVA), serotonin hydrochloride (5-HT), 3-methoxytyramine (3-MT), vanillylmandelic acid (VMA), epinephrine (EPI), dihydroxyphenylalanine (DOPA), 3-methoxy-4-hydroxyphenylglycol (MHPG), acetonitrile (Chromasolv Plus), monobasic sodium phosphate, ethylene-diamine-tetra-acetic acid (EDTA) disodium salt, 1-octanesulfonic acid (OSA) sodium salt, triethylamine (TEA), 85% phosphoric acid, 70% perchloric acid (PCA), and sodium bisulfite were purchased from SigmaAldrich. HPLC-grade water was produced using a Milli-Q Ultra-Pure water system (Merck Millipore).

Preparation of tissue samples: Ice-cold 0.1 M PCA was added to preweighed tissue samples at approximately 10–20 μl PCA per mg of tissue. Samples were then immediately homogenized using an ultrasonic processor (EpiShear Probe Sonicator; Active Motif) with a 3 mm probe at 20% amplitude for 6 s. Samples were incubated on ice for 10 min, vortexed and centrifuged at 16000 × *g* for 15 min at 4 °C. Resulting supernatants were transferred to centrifugal filter tubes with 0.2 μm nylon membrane inserts and centrifuged at 5000 × *g* for 3 min. Eluents were immediately stored at −80 °C and subjected to HPLC-ECD analysis within 6 days.

Standard solutions and calibration: Standard solutions of 3-MT, 5-HT, 5-HIAA, DA, DOPAC, DOPA, HVA, VMA, EPI, NA and MHPG were prepared at 500 μg/ml in 0.1 M PCA on the day before the assay. From these solutions, a mix containing all standards was prepared in 0.1 M PCA with a concentration of 10 μg/ml per standard, and this mix was stored as aliquots at −80 °C. On the next day, this mix was further diluted with 0.1 M PCA to obtain final standard concentrations of 200, 100, 50, 10, 5, 2 and 1 ng/ml. Calibration curves were obtained with the Chromeleon software through linear regression of peak area versus concentration. Coefficients of determination were 0.999.

Instrumentation and analysis: The HPLC-ECD system was a Dionex Ultimate 3000 series (all parts from Dionex, ThermoFisher Scientific) comprising an ISO-3100BM HPLC pump, WPS-3000TBSL analytical autosampler with temperature control, SRD-3200 solvent rack with built-in 2-channel vacuum degasser, Coulochem III detector with thermal organizer module, and a 5011A coulometric analytical cell. Analyte separation was performed on a Dionex C18 reversed-phase MD-150 3.2 mm × 150 mm column (3 μm particle size). Column and analytical cell were kept at 45 °C. The mobile phase, which was pumped at a flow rate of 0.5 ml/min, consisted of 75 mM monobasic sodium

phosphate, 3.1 mM OSA, 100 µl/l TEA, 25 µM EDTA and 10% acetonitrile (v/v), and was filtered through a nylon membrane (pore size 0.2 µm). The pH was adjusted to 3.0 with 85% phosphoric acid before degassing of the mobile phase for approximately 5 min and equilibration overnight on the HPLCECD system. For detection of neurotransmitters and metabolites, the first and second analytical cells were set to −100 mV and +300 mV, respectively. Processed tissue samples were thawed on ice in the dark for about 1 h before analysis, placed in the autosampler and kept at 5 °C before injection. Injection volume was 20 µl per sample. Chromatograms were acquired with Dionex Chromeleon 7 software over an acquisition time of 15 min. Analyte concentrations in tissue samples were expressed as ng/mg.

2.3. Experiments performed in normal GPR88 WT and KO mice 2.3.1. tacrine-induced tremulous jaw movements

To assess 3–7 Hz tremulous jaw movement, normal mice were treated with tacrine (2.5 mg/kg i.p.; Sigma). After 20 min, they were placed in a clean cage situated in an elevated position to allow complete observation of the experimental animal. After 10 min of habituation, tremulous jaw movements-defined as vertical and purposeless deflections of the lower jaw (Salamone et al., 2001) - were manually scored for 5 min. Yawns, tongue protrusions, and stereotypes, such as grooming, were not included in the evaluation.

2.3.1. Open-field test to measure locomotion activity

The test was performed for 30 min in a 46 × 46 cm^2 arena with grey floor and walls. The arena was illuminated by reflected light, providing an intensity of 30 lux on the floor of the arena. The arena was cleaned with 70% ethanol after each test session to eliminate olfactory cues. Video tracking was performed using a video camera mounted in the ceiling and analysed by EthoVision XT11.5 (Noduls) software.

2.3.2. FAST measurements of glutamate release

GPR88 WT or KO mice were anesthetized with isoflurane (3% for induction, 0.7–1% for maintenance) and mounted in a stereotaxic frame (David Kopf Instruments) fitted with a Cunningham mouse adapter (Stoelting Co.). Small cranial windows were drilled over the striatum (AP: +1.3; ML: ± 1.5; DV: −2.5 versus bregma), and microelectrode arrays (MEAs) were inserted into dorsal striatum of the intact and DA-depleted hemispheres. As previously described (Alvarsson et al., 2015; Stan et al., 2014; Hascup et al., 2008), glutamate dynamics were assessed on a subsecond timescale by MEA recordings with two of four electrode sites coated with L-glutamate oxidase enzyme, which breaks down L-glutamate into α-ketoglutarate and peroxide (H2O2). By using constant voltage amperometry with application of a fixed potential, the H2O2 was oxidized, with electron loss, and the resulting current was recorded using a Fast Analytical Sensing Technology-16 (FAST-16 MKII) electrochemistry instrument (Quanteon). Depolarization-induced glutamate release was induced by an isotonic solution of 70 mM KCl ejected for 1 s at 1 min intervals through a glass micropipette positioned at a distance of 50–100 µm from the MEA recording sites. For exogenously applied glutamate, 30 µM of glutamate was applied in the same way. A MATLAB graphic interface was used to calculate concentrations of glutamate from an average of 3–5 amplitudes per mouse. The area under curve (AUC) of the glutamate waveform, maximum amplitude of evoked glutamate (Evoked Glu, exclude amplitude less than 0.5 µM) and the decay time from maximum amplitude to 80% decay (T80) were measured. The tonic glutamate levels were determined as the current recorded on the sentinel sites subtracted from the current on the glutamate recording sites (Burmeister et al., 2002; Hascup et al., 2010).

2.4. Data analysis and statistics

Autoradiograms from ligand binding autoradiography and ISH experiments were digitized using a Dia-Scanner (Epson Perfection 4870 PHOTO). Optical density values were measured using Image J (1.52h, Wayne Rasband National Institutes of Health, USA). Statistical significance of the results was assessed by using Student's t-test for paired observations (comparisons with baseline within single groups) or three way ANOVA multiple comparison test followed by Fisher's LSD post hoc test. Pvalues, degrees of freedom and F values are detailed in the results part. For Student's t-test we used Graph Pad Prism 7.0. For three way ANOVA we used Stata 12.0. The individual group outliers were identified through quartile ± 1.5 interquartile range and removed.

3. Results

3.1. Unilaterally 6-OHDA-lesioned GPR88 KO mice make increased L-DOPA induced contralateral rotations but reduced abnormal involuntary movements

Our 6-OHDA MFB lesioning protocol causes near-complete reductions of DAT in both GPR88 WT and KO mice (Fig. 1A). The administration of L-DOPA to unilaterally 6-OHDA lesioned animals leads to contralateral rotations and abnormal involuntary movements (AIMs), behaviors which sensitize upon repeated L-DOPA treatment. Prior to

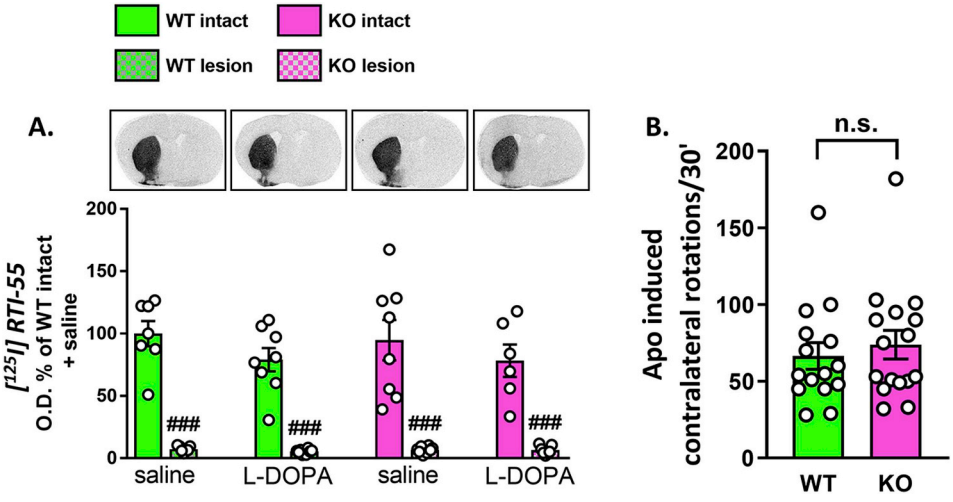

Fig. 1. Histological and behavioral evaluation of 6-OHDA lesion efficacy. (A) Histological validation of the 6-OHDA MFB lesion by using (125I) RTI-55 autoradiography (DAT-binding autoradiography). Bar graphs and representative autoradiographs for all the four groups. The 6-OHDA injection in MFB reduced significantly the (125I) RTI-55 binding signal over 90% of the WT intact side for all the groups. (B) Bar graph showing the number of apomorphine induced contralateral rotations in GPR88 WT (n = 15) and KO (n = 16) lesioned mice. Data are expressed as mean ± SEM. Three way ANOVA: treatment: $F(1, 51) = 2.51$, $p = 0.1191$; hemisphere: $F(1, 51) = 169.44$, $p < 0.0001$; treatment × hemisphere: $F(1, 51) = 1.97$, $p = 0.1660$; genotype: $F(1, 51) = 0.05$, $p = 0.8238$; treatment × genotype: $F(1, 51) = 0.06$, $p = 0.8013$; hemisphere × genotype: $F(1, 51) = 0.07$, $p = 0.7978$; treatment × hemisphere × genotype: $F(1, 51) = 0.01$, $p = 0.9158$. Intact vs lesion, ###$p < 0.001$, Fischer's LSD post hoc test. WT vs KO, n.s.: non-significant, $p > 0.05$, unpaired Student's t-test.

using this paradigm, unilaterally 6-OHDA lesioned GPR88 KO and WT mice were assessed by the number of apomorphine induced rotations and showed no genotype difference (Student's unpaired *t*-test, $p = 0.5713$; Fig. 1B). The therapeutic effect of L-DOPA is interpreted by measuring contralateral rotations while dyskinesia is assessed by the frequency of abnormal involuntary movements (AIMs) (Cenci et al., 1998). GPR88 WT and KO mice were thereafter treated repeatedly with L-DOPA and a two way ANOVA showed a significant difference in the contralateral rotational turns between the groups (Table S1). Post hoc analysis showed that administration of L-DOPA for 3 weeks led to a significant increased number of contralateral rotations within 30 min in both WT and KO animals (Fisher's LSD post hoc test: WT day 14 vs WT day 1, $p = 0.01$; WT day 21 vs WT day 1, $p < 0.0001$; KO day 14 vs KO day 1, $p = 0.0006$; KO day 21 vs KO day 1, $p < 0.0001$; Fig. 2A). The same post hoc test also revealed that during all the time points, GPR88 KO mice had significantly higher rotational rate than the WT mice (Fisher's LSD post hoc test: WT day 1 vs KO day 1, $p = 0.048$; WT day 7 vs KO day 7, $p = 0.0435$; WT day 14 vs KO day 14, $p = 0.0022$; WT day 21 vs KO day 21, $p = 0.0006$; Fig. 2A). Along with the enhanced L-DOPA induced rotational response, GPR88 KO mice showed considerably lower AIMs scores. A two way ANOVA revealed significant difference in the total number of AIMs (Table S1). A post hoc test showed that GPR88 KO mice exhibited significantly less AIMs than WT mice, on the 14th and 21st day of treatment (Fisher's LSD post hoc test: WT day 14 vs KO day 14, $p = 0.0001$; WT day 21 vs KO day 21, $p < 0.0001$; Fig. 2B). Furthermore, WT mice displayed significantly higher number of AIMs on 14th and 21st day compared with the 7th day (Fisher's LSD post hoc test: WT day 14 vs WT day 7, $p = 0.0003$; WT day 21 vs WT day 7, $p < 0.0001$; Fig. 2B). Conversely, GPR88 KO showed only significantly more AIMs on the 21st day when compared to the 7th day (Fisher's LSD post hoc test: KO day 21 vs KO day 7, $p = 0.0293$; Fig. 2B). Detailed subscore analyses of AIMs (Fig. 3A–D) with two way ANOVAs showed that axial and orofacial AIMs were significantly different among the genotypes and the time points (Table S2). The same test also showed that forelimb AIMs were significantly different only among the genotypes, while locomotive AIMs did not show any significant differences (Table S2).

3.2. Unilaterally 6-OHDA-lesioned GPR88 KO mice differentially regulates the mRNA of L-DOPA induced genes

As aforementioned, we observed that GPR88 KO mice simultaneously have augmented rotational behavior and diminished AIM scores in comparison with the WT mice. These distinct behavioral responses were not due to a differential neurotoxic response towards 6-OHDA as autoradiographic detection of DAT showed no genotype difference (Fig. 1A). To obtain insight in the molecular mechanisms underlying the beneficial L-DOPA responses in GPR88 KO mice, we decided to study selected mRNA changes in striatal sections from the same animals which had undergone the behavioral assessments upon chronic L-DOPA treatment. It has been determined that both acute and chronic L-DOPA treatments induce the mRNA expression of immediate early genes (IEGs), like cFOS, ARC and EGR-1 (Fisone and Bezard, 2011). Moreover, it is well-established that chronic LDOPA administration increases the transcription of PENK, PDYN and GAD67 mRNAs (Cenci et al., 1998; Picconi et al., 2018; Sgroi and Tonini, 2018). Furthermore, there are studies which state that contralateral rotations and AIMs are independently correlated with PDYN and PENK elevation respectively (Breger et al., 2013; Sgroi and Tonini, 2018). Based on these previous studies, we decided to perform experiments with 35 S labelled antisense probes towards ARC, PENK, PDYN and GAD67 mRNAs. Three way ANOVA showed significant difference of PDYN, GAD67 and ARC transcripts between the groups (Table S3). Post hoc analysis revealed that L-DOPA treated GPR88 KO mice had a smaller increase of PDYN and GAD67 mRNA than the WT (Fisher's LSD post hoc test: WT lesion LDOPA vs KO lesion L-DOPA, PDYN: $p < 0.0001$; Fig. 4A; GAD67: $p = 0.015$; Fig. 4C; ARC: $p < 0.0001$; Fig. 4D). Furthermore, post hoc analysis unveiled that GAD67 transcripts were significantly higher in the lesioned side of the L-DOPA treated WT animals while this effect was absent in the LDOPA treated KO mice (Fisher's LSD post hoc test: WT intact L-DOPA vs WT lesion L-DOPA, $p = 0.007$; KO intact L-DOPA vs KO lesion L-DOPA, $p = 0.185$; Fig. 4C). In contrast to the aforementioned genes, ARC mRNA was more increased in GPR88 KO than WT mice (Fisher's LSD post hoc test: WT lesion L-DOPA vs KO lesion L-DOPA, $p < 0.0001$; Fig. 4D). Moreover, three way ANOVA showed that PENK transcripts were significantly affected by the hemisphere factor (Table S3). Post hoc analysis revealed that PENK did not show any significant difference between GPR88 WT and KO mice (Fisher's LSD post hoc test: WT lesion L-DOPA vs KO lesion L-DOPA, $p = 0.349$; Fig. 4B). We used fluorescent ISH (RNAscope) with PDYN and ARC probes in 3 WT and 3 KO mice, to identify the ARC and PDYN positive cells in the L-DOPA treated lesioned striata (Fig. 4E). Approximately 90% of ARC positive cells express PDYN in both WT and KO mice (Cell type: $F(1,8) = 1844$, $p < 0.0001$; Genotype: $F(1,8) = 2.482$, $p = 0.1538$; Cell type × Genotype: $F(1,8) = 0.073$, $p = 0.79$) (Fig. 4F). Consequentlty, the neurons that show less PDYN in GPR88 KO mice than in WT animals are the same as those that have more transcripts of ARC. Taken together, our ISH data indicate that

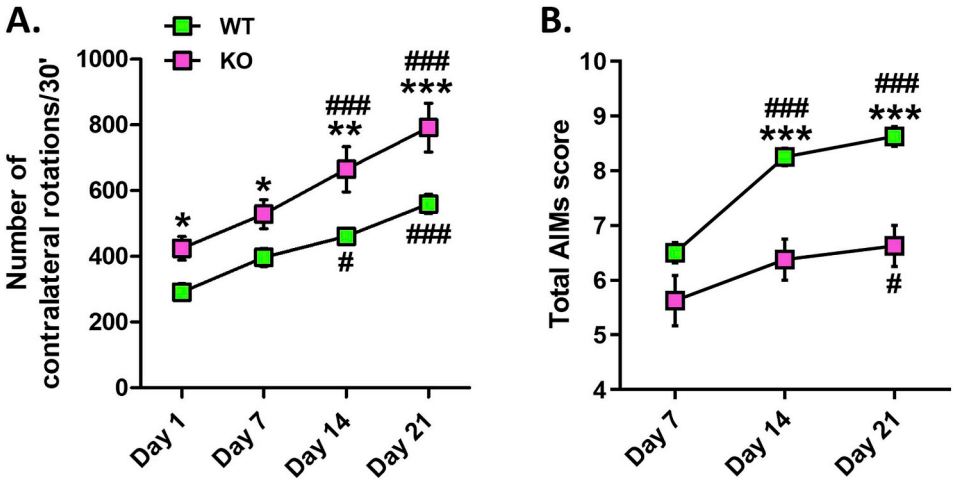

Fig. 2. GPR88 KO show low AIM score but increased contralateral rotations produced by chronic L-DOPA. (A, B) Line graphs representing the number of contralateral rotations and total AIMs in different time points of chronic L-DOPA administration. GPR88 KO (magenta, n = 8) had significantly higher rotational rate than the WT (green, n = 8) from the 1st till the 21st day of L-DOPA administration. Both GPR88 KO and WT showed significant rotation sensitization to L-DOPA at the 14th and 21st day. GPR88 KO mice had significantly fewer total AIMs than the WT on the 7th, 14th and 21st day of the treatment period. WT had significantly higher AIM score than 7th day in both 14th and 21st day. Whereas, KO had significantly more AIMs than the 7th day only during the 21st day of the treatment. Data are expressed as mean ± SEM. WT vs KO each time point, *p < 0.05; **p < 0.01; ***p < 0.001, Fischer's LSD post hoc test. Number of rotations for both WT and KO on Day 7, 14, 21 vs Day 1, #p < 0.05; ###p < 0.001, Fischer's LSD post hoc test. Number of AIMs for both WT and KO on Day 14, 21 vs Day 7, #p < 0.05; ###p < 0.001, Fischer's LSD post hoc test.

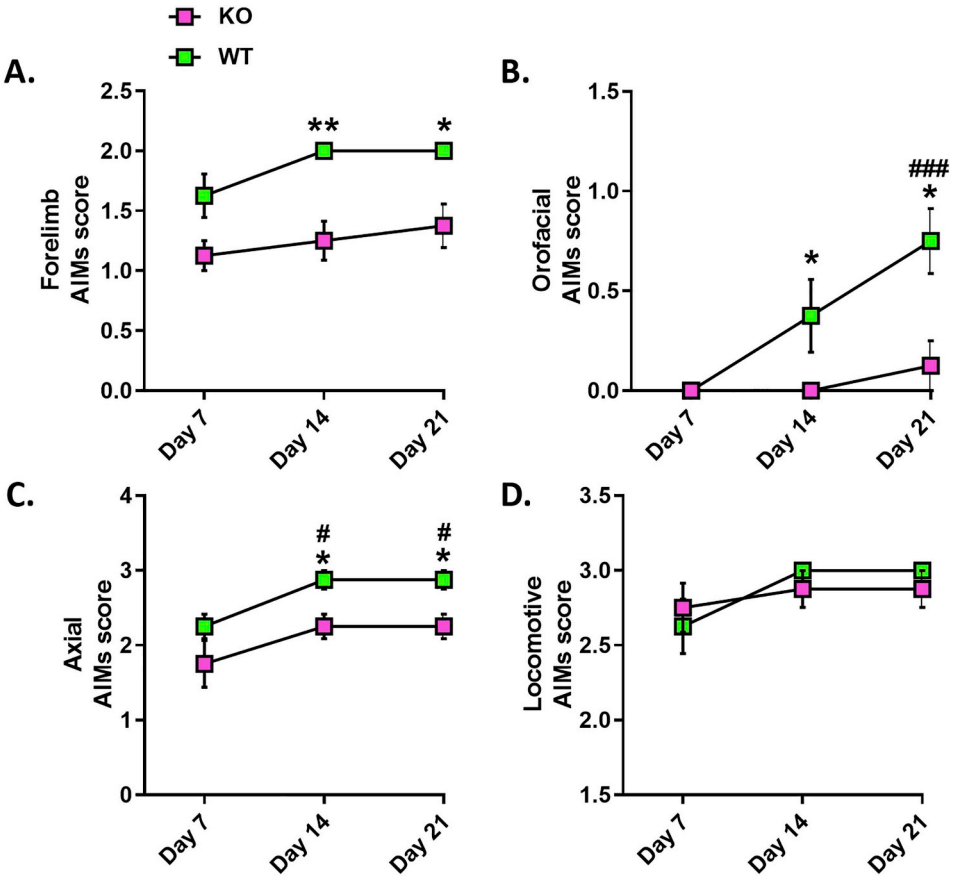

Fig. 3. GPR88 KO display less number of forelimb, axial and orofacial AIMs but not locomotor AIMs. (A–D) Line graphs depicting the number of forelimb (A), axial (B), orofacial (C) and locomotive (D) AIMs in the Day 7, 14 and 21 of chronic L-DOPA administration. GPR88 KO (magenta, n = 8) had significantly less forelimb, axial and orofacial AIMs than the WT (green, n = 8) in the 14th and the 21st day of the treatment. Data are expressed as mean ± SEM. WT vs KO, *p < 0.05; **p < 0.01, Fischer's LSD post hoc test. Number of AIMs for both WT and KO on Day 14, 21 vs Day 7, #p < 0.05; ###p < 0.001, Fischer's LSD post hoc test.

GPR88 KO mice display a lower upregulation of PDYN and GAD67 but a higher upregulation of ARC after L-DOPA administration.

3.3. GPR88 KO mice display altered levels of striatal 3-methyltyramine (3-MT) and 5hydroxytryptamine (5-HT)

To further investigate the mechanisms behind these behavioral aspects after the administration of LDOPA, we furthermore performed HPLC with focus on striatal monoamines and their metabolites. Three way ANOVA showed a significance between WT and KO only for 3-MT and 5-HT (Tables S4, S5, S6). Post hoc test revealed that GPR88 KO mice had lower 3-MT levels in the intact hemisphere (Fisher's LSD post hoc test: WT intact saline vs KO intact saline, p = 0.014). Moreover, L-DOPA increased the amount of 3-MT in the intact side of GPR88 KO mice (Fisher's LSD post hoc test: WT intact saline vs WT intact L-DOPA, p = 0.131; KO intact saline vs KO intact lesion, p = 0.026; Fig. 5A). This effect was not observed in WT mice (Fisher's LSD post hoc test: WT intact saline vs WT intact L-DOPA, p = 0.131; Fig. 5A). Post hoc test also revealed that GPR88 KO mice had lower 5HT than the WT, in the lesioned hemisphere (Fisher's LSD post hoc test: WT lesion saline vs KO lesion saline, p = 0.002; Fig. 5B). Moreover, the same test showed that 5-HT decreased after the administration of L-DOPA in the lesioned hemisphere of WT mice, while there was no effect in GPR88 deficient mice (Fisher's LSD post hoc test: WT lesion saline vs WT lesion L-DOPA, p = 0.014; KO lesion saline vs KO lesion L-DOPA, p = 0.085; Fig. 5B).

3.4. Normal GPR88 KO mice show increased locomotion and reduced tacrine-induced tremulous jaw movements

The total distance that GPR88 KO and WT mice moved in an open field was measured for 30 min. In accordance with previous studies (Maroteaux et al., 2018; Meirsman et al., 2016b, 2017; Quintana et al., 2012), GPR88 KO animals performed significantly longer paths within the field in comparison with the WT (Student's unpaired *t*-test: t (2.3), p = 0.03; Fig. 6A–C).

We studied the influence of GPR88 in PD-like induced tremor. The administration of tacrine, an acetylcholinesterase inhibitor, causes tremulous jaw movements (TJM) in a frequency which resembles that one of PD tremor (3–7 Hz) (Salamone et al., 2001). GPR88 KO animals had lower number of TJMs than the WT counterparts (Student's unpaired *t*-test: t (8.8), p < 0.0001, Fig. 6D).

3.5. Tonic and evoked glutamate release is elevated in striatum of normal GPR88 KO mice

Corticostriatal glutamate is known to have a central position in the motor sensitization towards dopaminomimetic compounds (Picconi et al., 2018; Duty, 2012; Johnson et al., 2009; Gerfen and Surmeier, 2011). By using in vivo FAST glutamate recording, we measured the amplitude of evoked and tonic release in dorsal striata from GPR88 WT and KO mice (Fig. 7A). Interestingly, we observed substantially increased glutamate striatal release in the GPR88 KO animals. There are higher concentration of both evoked and tonic glutamate release (Student's unpaired *t*-test, Evoked: t (3.8), p = 0.0010; Fig. 7B; Tonic: t (2.5), p = 0.0234; Fig. 7C). Moreover the AUC of the glutamate levels in GPR88 KO mice was larger than the one of the WT mice (Student's unpaired *t*-test, t (5.9), p < 0.0001; Fig. 7D). An increased AUC relies on higher peaks and on slower return to baseline. The slower decay of the glutamate signal is dependent on the clearance from the extracellular space. To quantify glutamate clearance we used the T80 time and found that it was significantly increased in the GPR88 KO striata compared to WT (Student's unpaired *t*-test, T80: t (2.8), p = 0.0101; Fig. 7E). It is known that astrocytes are largely responsible for removing synaptic glutamate, but GPR88 has not been detected in any glial cell

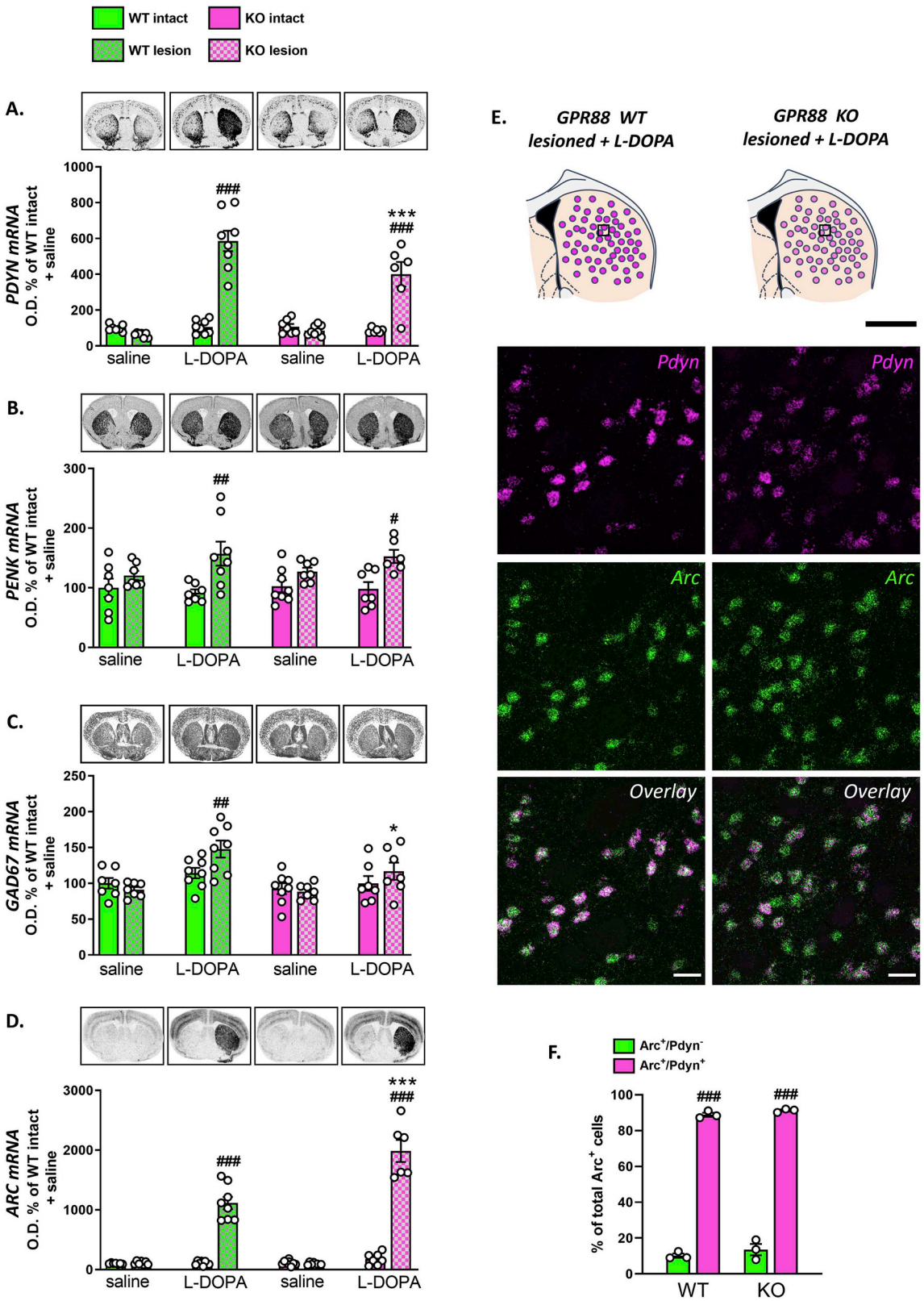

Fig. 4. GPR88 KO show altered L-DOPA induced transcription of PDYN, GAD67 and ARC. (A–D) Bar graphs and representative ISH autoradiographs for PDYN, PENK, GAD67 and ARC mRNAs (WT saline: n = 7, WT L-DOPA: n = 8, KO saline: n = 8, KO L-DOPA: n = 7). (A) GPR88 KO mice had significantly lower upregulation of PDYN than the WT. (B) Chronic L-DOPA treatment (21 days) significantly increased PENK in the lesioned striata of the WT but not of the KO. (C) GPR88 KO mice displayed significantly smaller enhancement of GAD67 than the WT. (D) ARC mRNA levels were significantly higher in GPR88 KO than their WT counterparts. (E) Representative FISH (RNAscope) images for PDYN-ARC (PDYN: magenta, PENK: green, ARC: white). (F) Bar graphs (WT: n = 3, KO: n = 3) showing the percentage of ARC+/PDYN- and ARC+/PDYN+ cells over the total ARC+ cells in the L-DOPA treated lesioned striata of WT and KO mice. Black scale bar: 1 mm. White scale bars: 30 μm. Data are expressed as mean ± SEM. WT lesion L-DOPA vs KO lesion LDOPA, *p < 0.05; **p < 0.01; ***p < 0.001, Fischer's LSD post hoc test. Intact L-DOPA vs lesion L-DOPA, #p < 0.05, ##p < 0.01, ###p < 0.001, Fischer's LSD post hoc test.

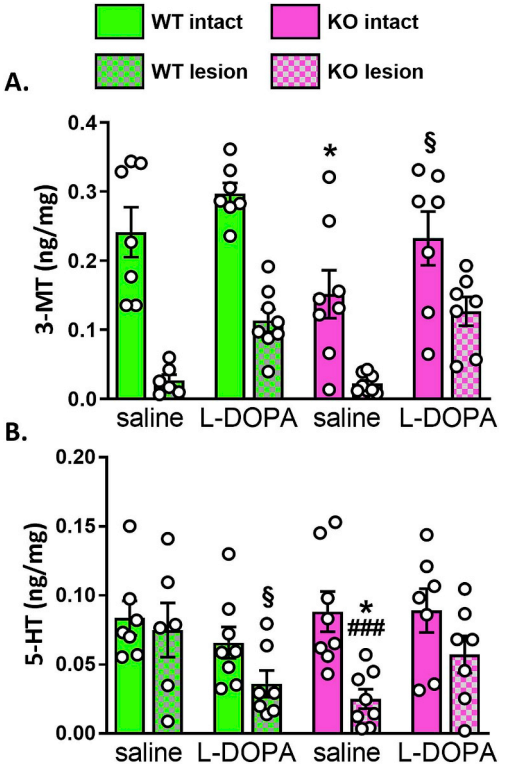

Fig. 5. GPR88 KO mice have altered striatal 3-MT and 5-HT. (A–B) Bar graphs showing the concentration of striatal 3-MT (A) and 5-HT (B) in lesioned GPR88 KO and WT mice after chronic LDOPA treatment (WT saline: n = 7, WT L-DOPA: n = 8, KO saline: n = 8, KO L-DOPA: n = 7). GPR88 KO mice have lower 3-MT than the WT in the intact side which is going back to WT levels after the administration of L-DOPA. 5-HT is negatively affected by the 6OHDA in GPR88 KO mice but not in the WT. L-DOPA reduces striatal 5-HT amount in the lesioned striata of WT mice but not in GPR88 KO. Data are expressed as mean ± SEM. WT vs KO, *p < 0.05, Fischer's LSD post hoc test. Intact vs lesion, ###p < 0.001, Fischer's LSD post hoc test. Saline vs LDOPA, §p < 0.05, Fischer's LSD post hoc test. Bars with grey outline: one outlier removed.

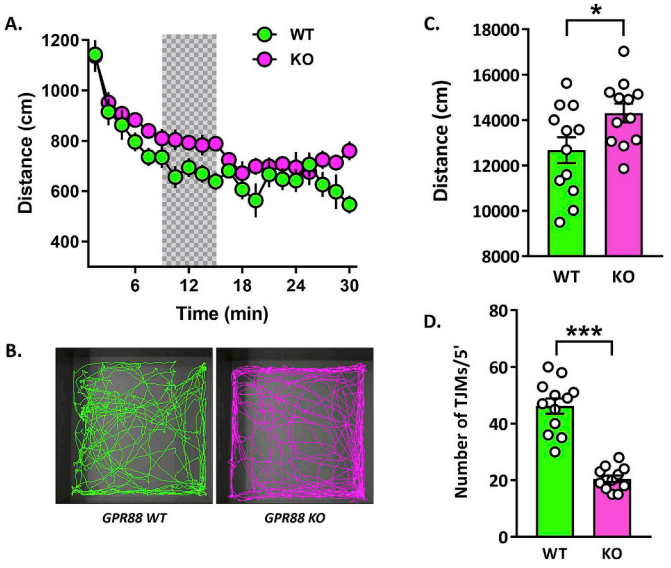

Fig. 6. GPR88 depletion induces hyperactivity and suppresses tacrine induced PD-like tremor. (A) Line graph showing the distance traveled (centimeters) in 90 s time bins over a 30 min period by GPR88 WT (n = 12) and KO (n = 12) mice. (B) Representative tracing of a GPR88 WT (green) and a KO (magenta) mouse movement during a period of 360 s which is denoted with grey box in the line graph of A. C. Bar graph depicting the total distance traveled (centimeters). (D) Bar graph showing the number of Tacrine-induced Jaw Movements (TJMs) over a period of 5 min. Data are expressed as mean ± SEM. *p < 0.05; **p < 0.01; ***p < 0.001, unpaired Student's t-test.

(Massart et al., 2009). We therefore hypothesized that the T80 rise depends upon the high wave peak amplitude. In order to test this hypothesis, we performed FAST recording in striata of GPR88 WT and KO animals by injecting glutamate solution without KCl (Fig. 7F). The exogenous application of glutamate gave rise to a glutamate wave that was similar in both GPR88 WT and KO (same peak amplitude and T80) (Student's unpaired *t*-test, Peak amplitude: t (0.14), p = 0.8873; Fig. 7G; t (0.01), AUC: p = 0.9918; Fig. 7H; t (0.5), T80: p = 0.6115; Fig. 7I). With this experiment, we confirmed that the increased T80 is an outcome from the high peak amplitude. Our findings indicate that GPR88 regulates the corticostriatal glutamate release.

4. Discussion

There are several possible explanations for the core observations that GPR88 KO mice display an enhanced rotational response to L-DOPA (related to potential therapeutic activity) whereas the induction of AIMS (a readout of potential induction of dyskinesia) is reduced. First, while both D1 and D2 agonism increase contralateral rotations, D2 agonists are less prone to develop AIMs (Carta et al., 2008; Schintu et al., 2016; Sgroi et al., 2016). Heightened L-DOPA-induced rotational response corresponds to therapeutical efficacy as it represents the locomotive induction by L-DOPA in the DA-depleted striatum (Lundblad et al., 2005). However, locomotive AIMs can be misleading due to their direct link with the rotational response (Lundblad et al., 2005). For this reason, there are studies that exclude locomotive AIMs when calculating the total AIM score (Lundblad et al., 2005). Previous studies have shown that GPR88 KO show higher sensitivity in MSNs' D2 receptors (Meirsman et al., 2017; Logue et al., 2009). This may then explain partially the heightened contralateral rotational rate without enhancement of AIMs, observed in GPR88 KO. Second, increased striatal expression of RGS4 mRNA after L-DOPA is positively correlated with the AIM score (Ko et al., 2014). Downregulation of RGS4 in GPR88 KO has previously been reported and may also account to their protective effect against AIMs (Quintana et al., 2012). Third, there is evidence that M4, which is a Gi muscarinic receptor, is inhibiting LIDs (Shen et al., 2015). Due to the Gi coupling of GPR88, KO mice may have higher baseline levels of cAMP that hamper the signaling of M4 upon activation (Jin et al., 2014).

In addition, at the cellular level, the present data are also in accordance with work showing that the occurrence of AIMs correlates with the levels of levels of PDYN and GAD67 in experimental parkinsonism (Cenci et al., 1998). Furthermore, our data reflected that the increased contralateral rotational rate of GPR88 KO are associated with the ARC mRNA levels. Interestingly, these transcriptional changes of PDYN and ARC in GPR88 KO striata are observed simultaneously on the same D1 MSNs. Both ARC and PDYN are upregulated by L-DOPA through cAMP/PKA/ERK pathway activation (Fisone and Bezard, 2011). Nevertheless, there are studies which show that the levels of cyclic nucleotides cAMP and cGMP are fluctuating in both hemispheres after the chronic treatment of L-DOPA (Giorgi et al., 2008; Sancesario et al., 2014). Specifically, there is a transient decrease of cAMP and cGMP during the peak of LIDs and a subsequent increase in the dyskinesiafree state (Sancesario et al., 2014). As GPR88 is a Gi coupled receptor, its absence may counteract such decrease of cAMP and cGMP levels in the dyskinetic phase. There is possibility that ARC and PDYN genes are differentially affected by the L-DOPA induced fluctuations of the cyclic nucleotides. Consequently, lack of GPR88 increases ARC and decreases PDYN, probably due to smaller reductions of cAMP/cGMP levels during L-DOPA treatment. These transcriptional alterations may lead to enhanced rotational rate and fewer number of AIMs

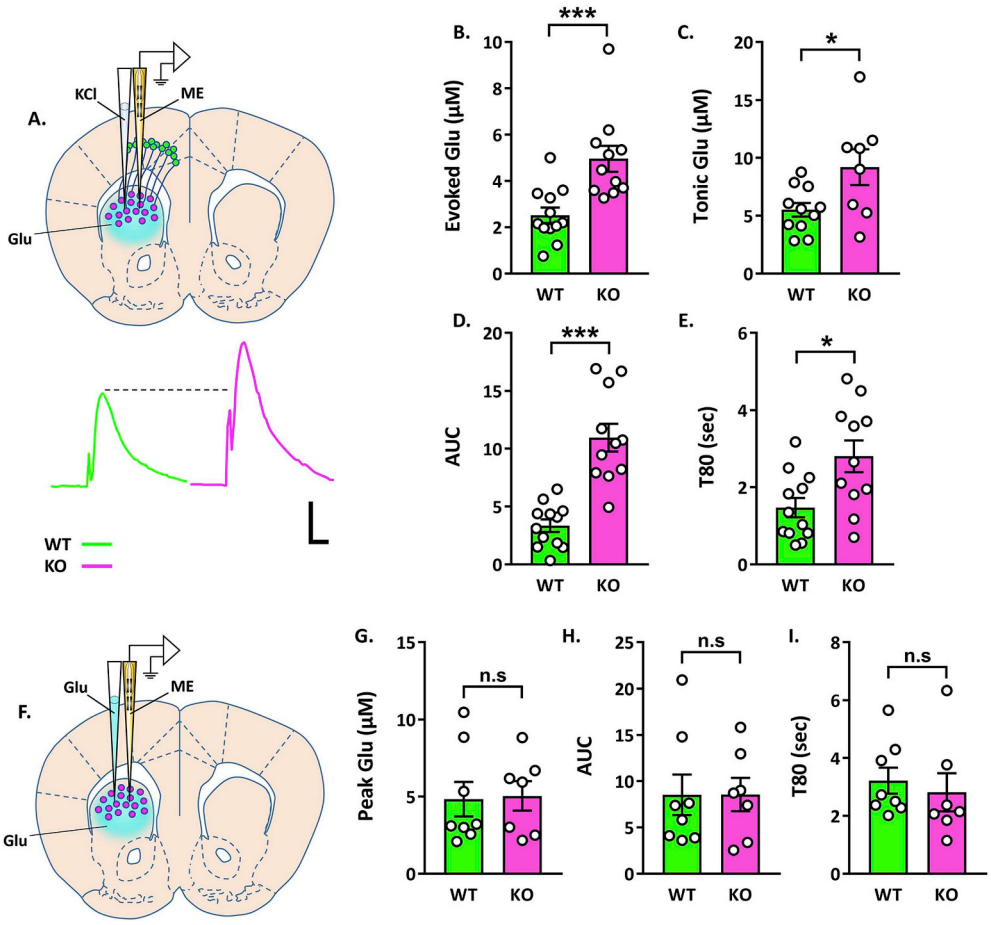

Fig. 7. GPR88 KO mice display high striatal glutamate release. (A) Schematic representation of the FAST recording in the dorsal striatum (cortical neurons: green, MSNs: magenta, KCl: depolarizing solution, ME: microelectrode, Glu: glutamate) and representative glutamate traces of a GPR88 WT (green) and a KO (magenta). Vertical scale bar: 1 μM, horizontal scale bar: 2.5 s. (B–E) Bar graphs (WT: n = 12, KO: n = 11) showing the evoked glutamate release concentration (B), the area under the curve (AUC) of the glutamate wave (C), the tonic glutamate release concentration (D) and the T80 (E). (F) Schematic representation of the FAST recording by using locally applied glutamate instead of depolarizing solution (MSNs: magenta, ME: microelectrode, Glu: glutamate). (G–I) Bar graphs (WT: n = 8, KO: n = 7) showing the peak concentration (G), the AUC (H) and the T80 (I) after the exogenous glutamate injection. Data are expressed as mean ± SEM. n.s.: non-significant, $p > 0.05$; *$p < 0.05$; **$p < 0.01$; ***$p < 0.001$, unpaired Student's t-test.

respectively.

In agreement with a role of GPR88 in 5-HT transmission, the present HPLC data indicate an additional mechanism whereby GPR88 may affect AIMs. GPR88 ISH data from the Allen brain atlas ISH database (image code: 79567811_149) denote the presence of GPR88 transcripts in dorsal raphe which is the major source of forebrain projecting 5-HT neurons. The pathophysiology of LID includes the displacement of 5-HT and release of "false" DA by serotoninergic terminals (Carta et al., 2007; Svenningsson et al., 2015; De Deurwaerdère et al., 2017). We could, indeed, find such a displacement of striatal 5-HT in the L-DOPA-treated WT mice. However, in GPR88 KO mice striatal 5-HT levels were unaffected by L-DOPA. Furthermore, we found significant reduced levels of 3-MT in intact striata of GPR88 KO mice which was normalized after L-DOPA administration. 3-MT is a catecholamine metabolite that occurs after the O-methylation of DA by catechol-O-methyl transferase (COMT) (Karoum et al., 1994). This reaction is considered to occur mostly in the extracellular space outside of DA neurons and reflects DA release rate (Karoum et al., 1994). It has been previously reported that GPR88 KO mice display lower striatal DA levels, which is in accordance with our results (Meirsman et al., 2016a). The alterations in DA metabolism in GPR88 KO mice may be adaptations to the aberrant intrinsic activity of MSNs and consequences on basal ganglia circuitry. The mechanism underlying this discrepancy remains to be studied, but it could underlie the reduced number of AIMs following L-DOPA in GPR88 KO mice.

Along with the potentiation of anti-parkinsonian action of L-DOPA in GPR88 KO mice, we found that these mice exhibits reduced PD-like tremor in response to tacrine. Tacrine is a potent acetylcholinesterase inhibitor which leads to an excess of striatal acetylcholine produced by the cholinergic interneurons (CINs) (Lehmann and Langer, 1983). The striatal expression of GPR88 is restricted to MSNs and is not found in CINs (Quintana et al., 2012; Massart et al., 2009), so we conclude that the tremor reducing actions in GPR88 KO mice are indirect. A possible D1-MSN hyperactivity and increased intracellular cAMP in GPR88 KO mice could counteract the inhibitory action of M4 cholinergic receptors which regulate tremor (Salamone et al., 2001; Oldenburg and Ding, 2011; Shen et al., 2015; Jin et al., 2014).

In line with previous work, it was observed that GPR88 KO mice had enhanced locomotor activity in an open field. GPR88 is confined on both types of MSNs, but previous studies have shown that deleting the receptor in D2-MSNs is adequate to produce a hyperactive phenotype (Meirsman et al., 2017). It has been observed that extracellular levels of DA are decreased in GPR88 KO mice (Meirsman et al., 2016a). Our HPLC results showed a significant decrease in striatal 3-MT of GPR88 KO, though DA and other DA metabolites where unchanged. Thus, the hyperactivity in the GPR88 KO mice is not associated with enhanced striatal levels of DA and its metabolites.

Since GPR88 KO mice appear to exhibit a DA-independent hyperlocomotion, we studied glutamate levels in these mice. Our data from striatal FAST recordings suggest that GPR88 is a negative regulator of glutamate release in striatum. This effect could be interpreted as the outcome of deletion of GPR88 either on corticostriatal neurons or MSNs. Electron microscopy studies have revealed that GPR88 is located in postsynaptic submembranous areas around the dendrites and within the nuclei (Massart et al., 2009, 2016). In the same studies no axonal GPR88 immunoreactivity was detected (Massart et al., 2009). ISH images from Allen Brain Atlas ISH database (image code: 79567811_357) show that GPR88 demonstrates notable expression levels in corticostriatal projection layers II/III and V. This cortical expression pattern on pyramidal neurons agrees with the data of previous studies (Sohur et al., 2014; Massart et al., 2016; Arefin et al., 2017; Ehrlich et al., 2018). As a consequence, the increased glutamate release

that we observe could be explained through the lack of an inhibitory influence of GPR88 on corticostriatal neurons. However, the predominance of GPR88 expression in striatum sets the possibility that the higher glutamate release also involves MSN derived mechanisms. Deletion of GPR88 affects the phosphorylation of GluR1 subunit, facilitating AMPA receptor activation, and the phosphorylation of DARPP-32 which are known to be crucial players for the long term potentiation (LTP) and depression (LTD) in MSNs (Quintana et al., 2012; Bateup et al., 2010; Calabresi et al., 2000; Huang, 1997). This process could involve several retrograde signaling molecules like nitric oxide, adenosine and endocannabinoids which regulate glutamate release (Huang, 1997; Bamford et al., 2018). With regards to endocannabinoid retrograde signaling, a critical molecule for their postsynaptic production is RGS4 (Lerner and Kreitzer, 2012). The reported lower striatal levels of RGS4 in GPR88 KO mice could lead to lower endocannabinoids and less retrograde inhibition of glutamate release (Lerner and Kreitzer, 2012; Quintana et al., 2012).

There is intense activity in developing ligands at GPR88. Recent studies have used a blood-brainbarrier permeable synthetic GPR88 agonist, RTI-13951-33, and showed beneficial actions against ethanol addiction in mice (Jin et al., 2016, 2018). Based on the current work it will be important to develop brain penetrant GPR88 antagonists to determine whether pharmacological blockade of GPR88 will promote anti-parkinsonian actions of L-DOPA while reducing its side effects.

5. Conclusion

Taken together, GPR88 KO mice exhibit increased basal locomotion, increased motor responsivity towards L-DOPA in the unilateral 6-OHDA lesion model and reduced tacrine-induced tremors. Meanwhile, GPR88 KO mice develop less AIMs in response to repeated L-DOPA. The graphical summary of our data is shown in Graphical Abstract. These data indicate that antagonism of GPR88 alone and/or in combination with L-DOPA may be useful for the symptomatic treatment of PD.

Acknowledgements

We thank Dr Ioanna Markaki for help with statistical analyses.

Appendix A. Supplementary data

Supplementary data to this article can be found online at https://doi.org/10.1016/j.neuropharm.2019.107829.

Funding and disclosures

This study was financially supported by the Karolinska Institutet-National Institute Health PhD programme, Konung Gustaf V och Drottning Victorias Frimurarestiftelse and Servier. Mark J Millan and Clotilde Manoury-la-cour are employees at Servier Research Institute. The other authors declare no competing interests.

References

Fisone, G., Bezard, E., 2011. Molecular mechanisms of L-DOPA-induced dyskinesia. Int. Rev. Neurobiol. 98, 95–122.
Alavi, M.S., Shamsizadeh, A., Azhdari-Zarmehri, H., Roohbakhsh, A., 2018. Orphan G protein-coupled receptors: the role in CNS disorders. Biomed. Pharmacother. 98, 222–232.
Alvarsson, A., Zhang, X., Stan, T.L., Schintu, N., Kadkhodaei, B., Millan, M.J., Perlmann, T., Svenningsson, P., 2015. Modulation by trace amine-associated receptor 1 of experimental Parkinsonism, L-DOPA responsivity, and glutamatergic neurotransmission. J. Neurosci. 35 (41), 14057–14069.
Arefin, T.M., Mechling, A.E., Meirsman, A.C., Bienert, T., Hübner, N.S., Lee, H.L., Ben Hamida, S., Ehrlich, A., Roquet, D., Hennig, J., von Elverfeldt, D., Kieffer, B.L., Harsan, L.A., 2017. Remodeling of sensorimotor brain connectivity in Gpr88-deficient mice. Brain Connect. 7 (8), 526–540.
Bamford, N.S., Wightman, R.M., Sulzer, D., 2018. Dopamine's effects on corticostriatal synapses during reward-based behaviors. Neuron 97 (3), 494–510.
Bateup, H.S., Santini, E., Shen, W., Birnbaum, S., Valjent, E., Surmeier, D.J., Fisone, G., Nestler, E.J., Greengard, P., 2010. Distinct subclasses of medium spiny neurons differentially regulate striatal motor behaviors. Proc. Natl. Acad. Sci. U. S. A. 107 (33), 14845–14850.
Bernheimer, H., Birkmayer, W., Hornykiewicz, O., Jellinger, K., Seitelberger, F., 1973. Brain dopamine and the syndromes of Parkinson and Huntington. Clinical, morphological and neurochemical correlations. J. Neurol. Sci. 20 (4), 415–455.
Bibbiani, F., Oh, J.D., Chase, T.N., 2001. Serotonin 5-HT1A agonist improves motor complications in rodent and primate parkinsonian models. Neurology 57 (10), 1829–1834.
Breger, L.S., Dunnett, S.B., Lane, E.L., 2013. Comparison of rating scales used to evaluate L-DOPAinduced dyskinesia in the 6-OHDA lesioned rat. Neurobiol. Dis. 50, 142–150.
Burmeister, J.J., Pomerleau, F., Palmer, M., et al., 2002. Improved ceramic-based multisite microelectrode for rapid measurements of L-glutamate in the CNS. J. Neurosci. Methods 119, 163171.
Calabresi, P., Gubellini, P., Centonze, D., Picconi, B., Bernardi, G., Chergui, K., Svenningsson, P., Fienberg, A.A., Greengard, P., 2000. Dopamine and cAMP-regulated phosphoprotein 32 kDa controls both striatal long-term depression and long-term potentiation, opposing forms of synaptic plasticity. J. Neurosci. 20 (22), 8443–8451.
Carta, M., Carlsson, T., Kirik, D., Björklund, A., 2007. Dopamine released from 5-HT terminals is the cause of L-DOPA-induced dyskinesia in parkinsonian rats. Brain 130 (Pt 7), 1819–1833.
Carta, A.R., Frau, L., Pontis, S., Pinna, A., Morelli, M., 2008. Direct and indirect striatal efferent pathways are differentially influenced by low and high dyskinetic drugs: behavioural and biochemical evidence. Park. Relat. Disord. 14 (Suppl. 2), S165–S168.
Cenci, M.A., Lee, C.S., Björklund, A., 1998. L-DOPA-induced dyskinesia in the rat is associated with striatal overexpression of prodynorphin- and glutamic acid decarboxylase mRNA. Eur. J. Neurosci. 10 (8), 2694–2706.
De Deurwaerdère, P., Di Giovanni, G., Millan, M.J., 2017. Expanding the repertoire of L-DOPA's actions: a comprehensive review of its functional neurochemistry. Prog. Neurobiol. 151, 57–100.
Duty, S., 2012. Targeting glutamate receptors to tackle the pathogenesis, clinical symptoms and levodopa-induced dyskinesia associated with Parkinson's disease. CNS Drugs 26 (12), 1017–1032.
Ehrlich, A.T., Semache, M., Bailly, J., Wojcik, S., Arefin, T.M., Colley, C., Le Gouill, C., Gross, F., Lukasheva, V., Hogue, M., Darcq, E., Harsan, L.A., Bouvier, M., Kieffer, B.L., 2018. Mapping GPR88-Venus illuminates a novel role for GPR88 in sensory processing. Brain Struct Funct. 223 (3), 1275–1296.
Gerfen, C.R., Surmeier, D.J., 2011. Modulation of striatal projection systems by dopamine. Annu. Rev. Neurosci. 34, 441–466.
Giorgi, M., D'Angelo, V., Esposito, Z., Nuccetelli, V., Sorge, R., Martorana, A., Stefani, A., Bernardi, G., Sancesario, G., 2008. Lowered cAMP and cGMP signalling in the brain during levodopa-induced dyskinesias in hemiparkinsonian rats: new aspects in the pathogenetic mechanisms. Eur. J. Neurosci. 28 (5), 941–950.
Hascup, K.N., Hascup, E.R., Pomerleau, F., Huettl, P., Gerhardt, G.A., 2008. Second-by-second measures of L-glutamate in the prefrontal cortex and striatum of freely moving mice. J. Pharmacol. Exp. Ther. 324 (2), 725–731.
Hascup, E.R., Hascup, K.N., Stephens, M., et al., 2010. Rapid microelectrode measurements and the origin and regulation of extracellular glutamate in rat prefrontal cortex. J. Neurochem. 115, 16081620.
Huang, E.P., 1997. Synaptic plasticity: a role for nitric oxide in LTP. Curr. Biol. 7 (3), R141–R143.
Hubbard, K.E., Wells, A., Owens, T.S., Tagen, M., Fraga, C.H., Stewart, C.F., 2010. Determination of dopamine, serotonin, and their metabolites in pediatric cerebrospinal fluid by isocratic high performance liquid chromatography coupled with electrochemical detection. Biomed. Chromatogr. 24 (6), 626–631.
Jin, C., Decker, A.M., Huang, X.P., Gilmour, B.P., Blough, B.E., Roth, B.L., Hu, Y., Gill, J.B., Zhang, X.P., 2014. Synthesis, pharmacological characterization, and structure-activity relationship studies of small molecular agonists for the orphan GPR88 receptor. ACS Chem. Neurosci. 5 (7), 576–587.
Jin, C., Decker, A.M., Harris, D.L., Blough, B.E., 2016. Effect of substitution on the aniline moiety of the GPR88 agonist 2-PCCA: synthesis, structure-activity relationships, and molecular modeling studies. ACS Chem. Neurosci. 7 (10), 1418–1432.
Jin, C., Decker, A.M., Makhijani, V.H., Besheer, J., Darcq, E., Kieffer, B.L., Maitra, R., 2018. Discovery of a potent, selective, and brain-penetrant small molecule that activates the orphan receptor GPR88 and reduces alcohol intake. J. Med. Chem. 61 (15), 6748–6758.
Johnson, K.A., Conn, P.J., Niswender, C.M., 2009. Glutamate receptors as therapeutic targets for Parkinson's disease. CNS Neurol. Disord. - Drug Targets 8 (6), 475–491.
Karoum, F., Chrapusta, S.J., Egan, M.F., 1994. 3-Methoxytyramine is the major metabolite of released dopamine in the rat frontal cortex: reassessment of the effects of antipsychotics on the dynamics of dopamine release and metabolism in the frontal cortex, nucleus accumbens, and striatum by a simple two pool model. J. Neurochem. 63 (3), 972–979.
Ko, W.K., Martin-Negrier, M.L., Bezard, E., Crossman, A.R., Ravenscroft, P., 2014. RGS4 is involved in the generation of abnormal involuntary movements in the unilateral 6-OHDA-lesioned rat model of Parkinson's disease. Neurobiol. Dis. 70, 138–148.
Lehmann, J., Langer, S.Z., 1983. The striatal cholinergic interneuron: synaptic tarhet of dopaminergic terminals? Neuroscience 10, 1105–1120.
Lerner, T.N., Kreitzer, A.C., 2012. RGS4 is required for dopaminergic control of striatal LTD and susceptibility to parkinsonian motor deficits. Neuron 73 (2), 347–359.
Logue, S.F., Grauer, S.M., Paulsen, J., Graf, R., Taylor, N., Sung, M.A., Zhang, L., Hughes, Z., Pulito, V.L., Liu, F., Rosenzweig-Lipson, S., Brandon, N.J., Marquis, K.L., Bates, B., Pausch, M., 2009. The orphan GPCR, GPR88, modulates function of the striatal

dopamine system: a possible therapeutic target for psychiatric disorders? Mol. Cell. Neurosci. 42 (4), 438–447.
Lundblad, M., Picconi, B., Lindgren, H., Cenci, M.A., 2004. A model of L-DOPA-induced dyskinesia in 6hydroxydopamine lesioned mice: relation to motor and cellular parameters of nigrostriatal function. Neurobiol. Dis. 16 (1), 110–123.
Lundblad, M., Usiello, A., Carta, M., Håkansson, K., Fisone, G., Cenci, M.A., 2005. Pharmacological validation of a mouse model of l-DOPA-induced dyskinesia. Exp. Neurol. 194 (1), 66–75.
Maroteaux, G., Arefin, T.M., Harsan, L.A., Darcq, E., Ben Hamida, S., Kieffer, B.L., 2018. Lack of anticipatory behavior in Gpr88 knockout mice showed by automatized home cage phenotyping. Genes Brain Behav., e12473.
Massart, R., Guilloux, J.P., Mignon, V., Sokoloff, P., Diaz, J., 2009. Striatal GPR88 expression is confined to the whole projection neuron population and is regulated by dopaminergic and glutamatergic afferents. Eur. J. Neurosci. 30 (3), 397–414.
Massart, R., Mignon, V., Stanic, J., Munoz-Tello, P., Becker, J.A., Kieffer, B.L., Darmon, M., Sokoloff, P., Diaz, J., 2016. Developmental and adult expression patterns of the G-protein-coupled receptor GPR88 in the rat: establishment of a dual nuclear-cytoplasmic localization. J. Comp. Neurol. 524 (14), 2776–2802.
Meirsman, A.C., Le Merrer, J., Pellissier, L.P., Diaz, J., Clesse, D., Kieffer, B.L., Becker, J.A., 2016a. Mice lacking GPR88 show motor deficit, improved spatial learning, and low anxiety reversed by delta opioid antagonist. Biol. Psychiatry 79 (11), 917–927.
Meirsman, A.C., Robé, A., de Kerchove d'Exaerde, A., Kieffer, B.L., 2016b. GPR88 in A2AR neurons enhances anxiety-like behaviors. eNeuro 3 (4).
Meirsman, A.C., de Kerchove d'Exaerde, A., Kieffer, B.L., Ouagazzal, A.M., 2017. GPR88 in A(2A) receptor-expressing neurons modulates locomotor response to dopamine agonists but not sensorimotor gating. Eur. J. Neurosci. 46 (4), 2026–2034.
Mizushima, K., Miyamoto, Y., Tsukahara, F., Hirai, M., Sakaki, Y., Ito, T., 2000. A novel G-protein-coupled receptor gene expressed in striatum. Genomics 69 (3), 314–321.
Oldenburg, I.A., Ding, J.B., 2011. Cholinergic modulation of synaptic integration and dendritic excitability in the striatum. Curr. Opin. Neurobiol. 21 (3), 425–432.
Paxinos, G., Franklin, K.B.J., 2001. The Mouse Brain in Stereotaxic Coordinates. Academic, San Diego.
Picconi, B., Hernández, L.F., Obeso, J.A., Calabresi, P., 2018. Motor complications in Parkinson's disease: striatal molecular and electrophysiological mechanisms of dyskinesias. Mov. Disord. 33 (6), 867–876.
Poewe, W., Seppi, K., Tanner, C.M., Halliday, G.M., Brundin, P., Volkmann, J., Schrag, A.E., Lang, A.E., 2017. Parkinson disease. Nat Rev Dis Primers 3, 17013.
Postuma, R.B., Berg, D., Stern, M., Poewe, W., Olanow, C.W., Oertel, W., Obeso, J., Marek, K., Litvan, I., Lang, A.E., Halliday, G., Goetz, C.G., Gasser, T., Dubois, B., Chan, P., Bloem, B.R., Adler, C.H., Deuschl, G., 2015. MDS clinical diagnostic criteria for Parkinson's disease. Mov. Disord. 30 (12), 1591–1601.
Quintana, A., Sanz, E., Wang, W., Storey, G.P., Güler, A.D., Wanat, M.J., Roller, B.A., La Torre, A., Amieux, P.S., McKnight, G.S., Bamford, N.S., Palmiter, R.D., 2012. Lack of GPR88 enhances medium spiny neuron activity and alters motor- and cue-dependent behaviors. Nat. Neurosci. 15 (11), 1547–1555.
Rainwater, A., Sanz, E., Palmiter, R.D., Quintana, A., 2017. Striatal GPR88 modulates foraging efficiency. J. Neurosci. 37 (33), 7939–7947.
Salamone, J.D., Correa, M., Carlson, B.B., Wisniecki, A., Mayorga, A.J., Nisenbaum, E., Nisenbaum, L., Felder, C., 2001. Neostriatal muscarinic receptor subtypes involved in the generation of tremulous jaw movements in rodents implications for cholinergic involvement in parkinsonism. Life Sci. 68 (2223), 2579–2584.
Sancesario, G., Morrone, L.A., D'Angelo, V., Castelli, V., Ferrazzoli, D., Sica, F., Martorana, A., Sorge, R., Cavaliere, F., Bernardi, G., Giorgi, M., 2014. Levodopa-induced dyskinesias are associated with transient down-regulation of cAMP and cGMP in the caudate-putamen of hemiparkinsonian rats: reduced synthesis or increased catabolism? Neurochem. Int. 79, 44–56.
Schintu, N., Zhang, X., Alvarsson, A., Marongiu, R., Kaplitt, M.G., Greengard, P., Svenningsson, P., 2016. p11 modulates L-DOPA therapeutic effects and dyskinesia via distinct cell types in experimental Parkinsonism. Proc. Natl. Acad. Sci. U. S. A. 113 (5), 1429–1434.
Schober, A., 2004. Classic toxin-induced animal models of Parkinson's disease: 6-OHDA and MPTP. Cell Tissue Res. 318 (1), 215–224.
Sgroi, S., Tonini, R., 2018. Opioidergic modulation of striatal circuits, implications in Parkinson's disease and levodopa induced dyskinesia. Front. Neurol. 9, 524.
Sgroi, S., Capper-Loup, C., Paganetti, P., Kaelin-Lang, A., 2016. Enkephalin and dynorphin neuropeptides are differently correlated with locomotor hypersensitivity and levodopa-induced dyskinesia in parkinsonian rats. Exp. Neurol. 280, 80–88.
Shen, W., Plotkin, J.L., Francardo, V., Ko, W.K., Xie, Z., Li, Q., Fieblinger, T., Wess, J., Neubig, R.R., Lindsley, C.W., Conn, P.J., Greengard, P., Bezard, E., Cenci, M.A., Surmeier, D.J., 2015. M4 muscarinic receptor signaling ameliorates striatal plasticity deficits in models of L-DOPA-induced dyskinesia. Neuron 88 (4), 762–773.
Sohur, U.S., Padmanabhan, H.K., Kotchetkov, I.S., Menezes, J.R., Macklis, J.D., 2014. Anatomic and molecular development of corticostriatal projection neurons in mice. Cerebr. Cortex 24 (2), 293–303.
Stan, T.L., Alvarsson, A., Branzell, N., Sousa, V.C., Svenningsson, P., 2014. NMDA receptor antagonists ketamine and Ro25-6981 inhibit evoked release of glutamate in vivo in the subiculum. Transl. Psychiatry 4, e395.
Svenningsson, P., Nomikos, G.G., Ongini, E., Fredholm, B.B., 1997. Antagonism of adenosine A2A receptors underlies the behavioural activating effect of caffeine and is associated with reduced expression of messenger RNA for NGFI-A and NGFI-B in caudate-putamen and nucleus accumbens. Neuroscience 79 (3), 753–764.
Svenningsson, P., Rosenblad, C., Af Edholm Arvidsson, K., Wictorin, K., Keywood, C., Shankar, B., Lowe, D.A., Björklund, A., Widner, H., 2015. Eltoprazine counteracts L-DOPA-induced dyskinesias in Parkinson's disease: a dose-finding study. Brain 138 (Pt 4), 963–973.
Ungerstedt, U., Arbuthnott, G.W., 1970. Quantitative recording of rotational behavior in rats after 6-hydroxy-dopamine lesions of the nigrostriatal dopamine system. . 1970 Dec 18;24(3):485-93. Brain Research 24 (3), 485–493.
Yang, L., Beal, M.F., 2011. Determination of neurotransmitter levels in models of Parkinson's disease by HPLC-ECD. Methods Mol. Biol. 793, 401–415.
Zhang, X., Andren, P.E., Greengard, P., Svenningsson, P., 2008. Evidence for a role of the 5-HT1B receptor and its adaptor protein, p11, in L-DOPA treatment of an animal model of Parkinsonism. Proc. Natl. Acad. Sci. U. S. A. 105 (6), 2163–2168.